Effect of asiaticoside for wound repair and fabrication of 3D biodegradable polymer mesh containing asiaticoside

Jeonghyun Lee

Department of Medical Science
The Graduate School, Yonsei University

Effect of asiaticoside for wound repair and fabrication of 3D biodegradable polymer mesh containing asiaticoside

Directed by Professor Jong-Chul Park

The Master's Thesis
Submitted to the Department of Medical Science,
the Graduate School of Yonsei University
in partial fulfillment of the requirements for the degree of
Master of Medical Science

Jeonghyun Lee

June 2012

This certifies that the Master's thesis
of Jeonghyun Lee is approved.

Thesis supervisor: Jong-Chul PARK

Thesis Committee Member#1: Dong-Wook HAN

Thesis Committee Member#2: Jeon-Soo SHIN

The Graduate School
Yonsei University

June 2012

Acknowledgements

저에게 2 년간의 석사생활은 노력과 열정을 배운 시기였습니다. 즐거운 시간, 힘든 시기 모두 지나 보내고, 제가 더욱 단단해 질 수 있도록 저에게 보이지 않게 많은 도움 주셨던 모든 분들께 감사 드립니다.

먼저 부족한 저를 받아 주시고 따뜻한 보살핌과 지도로 이끌어 주신 박종철 교수님께 감사 드립니다. 교수님의 가르침을 따라 바른 연구자의 길을 가도록 하겠습니다. 그리고 저의 졸업을 위해 바쁘신 와중에도 매번 귀한 시간 내어주셨던 신전수 교수님, 학부시절부터 언제나 아낌없는 지도와 격려해주신 한동욱 교수님께도 마음속 깊이 감사 드립니다.

동고동락하며 정말 많은 추억을 쌓았던 우리 실험실 식구들에게도 고맙다는 말을 전하고 싶습니다. 모두를 두루 보살펴 주시는 사려 깊은 현숙언니, 놀라운 동안 미모의 소유자 태화언니, 돌아와서 정말 반가운 착한 대형오빠, 축구와 음악을 좋아하는 현용오빠, 2 년 동안 정말 많은 도움 주셨던 고마운 미희언니, 저를 위한 많은 가르침 주셨던 혜리언니, 함께 있으면 항상 즐거운 상냥한 병주언니, 진지한 듯 재미있는 배려 깊은 혁진오빠, 보기만 해도 웃긴 유쾌한 민성오빠, 언제나 열심인 귀여운 우리 할매 경은언니, 고양이 같은 조용한 관찰자 귀여운 민아, 이제는 혜자가 편한 평화의 상징 나의 재미 혜진, 털털한 성격의 동갑내기 민현, 지금은 졸업했지만 보고 싶은 재경언니, 바보라언니까지 모두 고맙고 소중한 인연들 입니다.

자주 보지는 못해도 항상 든든하게 느껴지는, 만난 지 어느덧 10 년이 넘은 내 친구들 진아, 주래, 선영, 영순, 유진, 그리고 재남이 (모두 본명이 낯설구나, 우리의 얕은 우정 영원히 함께 하자!), 재미진 추억만 한 가득한 기영 그리고 영은, 연주 (보고싶다!), 힘들었던 고 3 시절 함께 보냈던, 똑똑이 내 친구들 생활관 패밀리 한송, 제하, 혜진, 혜경, 혜민이 (모두 잘 돼서 매우 기분 좋다!), 질풍노도 스무 살에 함께 진로를 고민했던, 지금은 각자의 위치에서 멋지게 살아가고 있는 나노 패밀리 은영, 용숙, 수정, 소영, 가영언니, 란언니까지 지금의 저를 있게 한 모든 인연에 감사합니다.

그리고 사랑하는 나의 가족! 할아버지, 할머니 오래오래 건강하세요, 사랑합니다. 존경하고 사랑하는 아빠, 엄마. 표현은 잘 못했지만 언제나 감사한 마음으로 살아가고 있습니다. 제가 가졌던 많은 행복들은 모두 부모님께서 베풀어주신 사랑으로 누릴 수 있었다고 생각해요. 그리고 회사 생활하느라 나랑 생활하느라 여러모로 바쁘고 고생이 많은 착한 우리 오빠에게도 고맙다고 말하고 싶습니다.

마지막으로 나를 완전히 이해하는 한 사람, 나의 연인에게 감사의 인사를 전합니다.

2012 년 6 월

이정현 드림

TABLE OF CONTENTS

ABSTRACT…… 1

I. INTRODUCTION..... 3

1. Skin..... 3
2. Cutaneous wound repair..... 4
3. Asiaticoside..... 6
4. Scaffold for tissue engineering..... 8
5. Objectives of the study..... 8

II. MATERIALS AND METHODS..... 9

1. Cells and cell culture conditions..... 9
2. Asiaticoside treatment method..... 9
3. Cell viability assay..... 9
4. Cell migration assay..... 10
5. Cell attachment assay..... 12
   - A. MTT assay..... 12
   - B. Fluorescent staining..... 12
   - C. Adhesion molecule observation..... 12
6. Cell proliferation assay..... 13
   - A. MTT assay..... 13
   - B. BrdU assay..... 13
7. Fabrication of 3D PLGA mesh..... 13
8. Asiaticoside-containing 3D PLGA mesh..... 16
   - A. Fabrication of asiaticoside-containing 3D PLGA mesh..... 16
   - B. Release pattern of asiaticoside-containing 3D PLGA mesh..... 16
   - C. Cytotoxicity of asiaticoside-containing 3D PLGA mesh..... 16
   - D. Attachment effect of asiaticoside-containing 3D PLGA mesh..... 17
   - E. Growth rate effect of asiaticoside-containing 3D PLGA mesh..... 17
9. Statistical analysis..... 17

III. RESULTS..... 18

1. Cell viability assay..... 18
2. Cell migration assay..... 20
3. Cell attachment assay..... 22

A. MTT assay & Fluorescent staining 22
B. Adhesion molecule observation 24
4. Cell proliferation assay 26
5. Fabrication of 3D PLGA mesh 28
6. Asiaticoside-containing 3D PLGA mesh 30
A. Fabrication of asiaticoside-containing 3D PLGA mesh 30
B. Release pattern of asiaticoside-containing 3D PLGA mesh 32
C. Cytotoxicity of asiaticoside-containing 3D PLGA mesh 34
D. Attachment effect of asiaticoside-containing 3D PLGA mesh on aHDFs 36
E. Growth rate effect of asiaticoside-containing 3D PLGA mesh 38

IV. DISCUSSION 40
V. CONCLUSION 42
REFERENCES 43
ABSTRACT (IN KOREAN) 46
PUBLICATION LIST 48

LIST OF FIGURES

Figure 1. Mechanism of cutaneous wound repair 5
Figure 2. Molecular structure of asiaticoside 7
Figure 3. Schematic of cell migration assay..... 11
Figure 4. Schematic of low temperature electrospinning..... 15
Figure 5. Effect of asiaticoside on the viability of aHDFs and aNHEKs..... 19
Figure 6. Effect of asiaticoside on the migration of aHDFs and aNHEKs..... 21
Figure 7. Effect of asiaticoside on the attachment of aHDFs and aNHEKs..... 23
Figure 8. Effect of asiaticoside on the adhesion molecule expression of aHDFs..... 25
Figure 9. Effect of asiaticoside on the proliferation of aHDFs and aNHEKs 27
Figure 10. Morphology of PLGA mesh fabricated at room temperature and low temperature 29
Figure 11. Morphology of fabricated 3D PLGA mesh containing asiaticoside 31
Figure 12. Release pattern of asiaticoside from asiaticoside-containing 3D PLGA mesh..... 33
Figure 13. Cytotoxicity of asiaticoside-containing 3D PLGA mesh against aHDFs 35
Figure 14. Effect of asiaticoside-containing 3D PLGA mesh on the attachment of aHDFs..... 37
Figure 15. Effect of asiaticoside-containing 3D PLGA mesh on the proliferation of aHDFs..... 39

ABSTRACT

Effect of asiaticoside for wound healing and
fabrication of 3D biodegradable polymer mesh containing asiaticoside

Jeonghyun Lee

Department of Medical Science
The Graduate School,Yonsei University

(Directed by Professor Jong-Chul Park)

Wound healing proceeds through a complex collaborative process involving many types of cells. Keratinocytes and fibroblasts of epidermal and dermal layers of the skin play prominent roles in this process. Asiaticoside, an active component of *Centella asiatica*, is known for its beneficial effects on keloid and hypertrophic scar. However, the effects of this compound on normal human skin cells are not yet firmly established. Using *in vitro* systems, we observed the effects of asiaticoside on normal human skin cell behaviors related to healing. In a wound closure seeding model, asiaticoside increased migration rates of skin cells. By observing the numbers of cells attached and the area occupied by the cells, we concluded that asiaticoside also enhanced the initial skin cell adhesion. In cell proliferation assays, asiaticoside induced an increase in the number of normal human dermal fibroblasts.

In the treatment of extensive full thickness burns, dermal replacements substitute the injured tissue. Polymer scaffolds with easy fabrication and reasonable price are widely used for

the dermal replacements. For the fabrication of poly(D,L-lactide-co-glycolide) (PLGA) mesh having porous 3D structure, the electrospinning method was carried out. The results indicated that the fabrication of scaffolds having sufficient thickness to replace a damaged tissue was possible by using low temperature electrospinning method. Asiaticoside was applied to the polymer scaffolds to increase biocompatibility of the scaffolds and to help tissue regeneration. Finally, the effects of 3D PLGA mesh containing asiaticoside on human dermal fibroblasts were evaluated as the possible use for dermal replacement and it showed enhanced cell adhesion and proliferation rate compared with a control.

In conclusion, asiaticoside promotes skin cell behaviors involved in wound healing; and as a bioactive component of an artificial skin, may have therapeutic value.

Key words: cutaneous wound repair, bioactive compounds, asiaticoside, fibroblast, keratinocyte, cell behavior, artificial skin

Effect of asiaticoside for wound healing and fabrication of 3D biodegradable polymer mesh containing asiaticoside

Jeonghyun Lee

Department of Medical Science
The Graduate School,Yonsei University

(Directed by Professor Jong-Chul Park)

I. INTRODUCTION

1. Skin

Skin is the largest organ in the body comprising approximately 15% of body weight, with epidermis, dermis and the subcutaneous layer included. Epidermis, the outermost layer of the skin, maintains a vital barrier against external insults. Dermis, the layer between the epidermis and subcutaneous tissue, endows the skin with firmness, elasticity and strength, and also regulates body temperature through control of blood flow and sweating. Keratinocytes comprise 95% of epidermis as the major cellular constituent, and fibroblasts predominate among cell types in the dermis[1,2].

2. Cutaneous wound repair

Wound healing spans several complicated phases, including inflammation, granulation and re-epithelialization (new tissue formation), contraction and remodeling of tissues[3] (Figure 1). Soon after wounding, cytokines attract inflammatory cells to remove damaged tissues and foreign substances. As inflammation subsides, fibroblasts and keratinocytes migrate into the wound area, adhere and proliferate to form new tissue. In this phase, changes in gene expression and phenotype guide the proliferation, migration and differentiation of keratinocytes and fibroblasts. New tissue formation begins with the migration of keratinocytes over injured dermis followed by capillary formation to support fibroblasts and macrophages as these cells replace the fibrin clot with granulation tissue. A second wave of keratinocytes will use the granulation tissue as a substrate[4,5]. Fibroblasts also compensate for lost tissue and protect the wound area from intrusion by debris. During re-epithelialization, keratinocytes proliferate and differentiate to restore function to the epithelium as a barrier against external conditions. Wound repair concludes through contraction of the wound site and tissue remodeling through differentiation and programmed cell death. Cutaneous wound healing is important for both medical and esthetic reasons and a large number of bioactive compounds have been tested for capacity to promote this process[6-8].

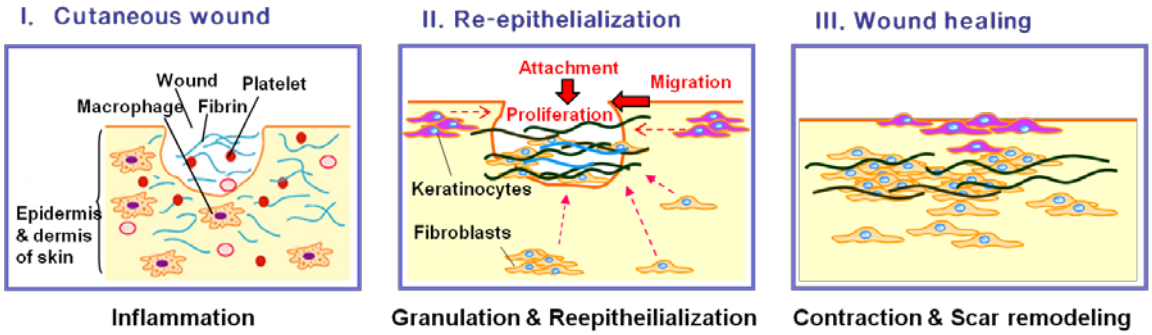

Figure 1. Mechanism of cutaneous wound repair. Skin cell behaviors have important role in tissue regeneration. During the wound healing, dermal fibroblasts and epidermal keratinocytes starts to migrate into the wound area, and attach and proliferate for granulation and re-epithelialization. Granulation and re-epithelialization protect wound sites from external environment and lead to tissue regeneration.

3. Asiaticoside

Centella asiatica has a long history of use in Asia for treating skin and vascular disease. Active components derived from the leaves of this small flowering plant, include asiaticoside, asiatic acid, madecassic acid and other compounds not yet identified. Among these components, asiaticoside displays the highest activity, as observed in the healing of gastric ulcer, leprosy and certain types of tuberculosis[9-11]. Molecular structure of asiaticoside is shown in Figure 2. Molecular formula and molecular weight of asiaticoside is $C_{48}H_{78}O_{19}$ and 959.12 respectively. Asiaticoside may also inhibit proliferative activity related to keloid and hypertrophic scar. The effects of asiaticoside on skin disorders such as keloid and hypertrophic scar have been studied in vitro and in vivo[12-14]; however, studies have not yet clearly defined the effects of asiaticoside on normal skin cells in wound healing.

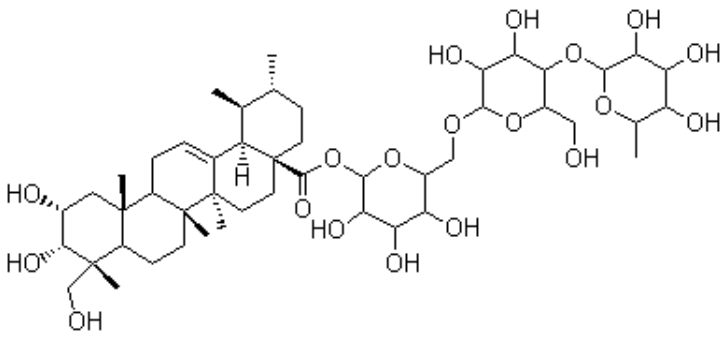

Figure 2. Molecular structure of asiaticoside. Molecular formula and molecular weight of asiaticoside is $C_{48}H_{78}O_{19}$ and 959.12 respectively.

4. Scaffold for tissue engineering

For the treatment of severe full thickness burn, dermal replacements are in use. Among the replacements, scaffolds of bovine collagen and allografts using donor's skin graft have been widely used for the regeneration of wound site. They have been showed outstanding results on clinical trials, but still have some limitations. In case of scaffolds made with bovine collagen, the clinical use of bovine-derived products have been considered to be avoided for the risk of bovine spongiform encephalitis. Allografts have the problems of expense and supply because many patients and surgeons tend to consider allografts only in life-threatening conditions.

Polymer scaffolds with high biocompatibility could be promising materials for tissue repair because of their reasonable price and easy fabrication for a stable supply. Scaffolds protecting the injured tissue and helping regeneration are required to have passages for the fluid exchange and the infiltration, migration, and attachment of cells. To satisfy the requirements, scaffolds with porous structures are necessary.

Electrospinning is one of the techniques used for the manufacture of porous scaffolds with fibrous structure similar to extracellular matrix of skin. However, electrospinning method has difficulties in the fabrication of scaffolds having sufficient thickness to replace injured skin. Recently, low temperature electropinning method using dryice has been introduced for 3-dimesional polymer mesh showing sufficient thickness.

5. Objectives of the study

The aim of this study is to evaluate the effects of asiaticoside on behaviors of normal human skin cells as a natural pharmaceutics for wound healing. The effects of asiaticoside to stimulate migration, initial attachment and proliferation of skin cells were examined. Also, we tried to find out the effects of asiaticoside on the behaviors of skin cells if it was introduced to the polymer scaffolds and therefore the effects of 3D PLGA mesh containing asiaticoside on human dermal fibroblasts were evaluated as the implications for dermal replacements.

II. MATERIALS AND METHODS

1. Cells and cell culture conditions

Adult human dermal fibroblasts (aHDFs) were purchased from Lonza Group, Ltd. (Walkersville, MD, USA) and maintained in fibroblast basal medium-2 (FBM-2) supplemented with growth kit (10 ml of fetal bovine serum, 0.5 ml of insulin, 0.5 ml of gentamicin sulfate amphotericin-B (GA-1000) and 0.5 ml of r-human fibroblast growth factor-B, Lonza). Adult normal human epidermal keratinocytes (aNHEKs) were purchased from Lonza and maintained in keratinocyte basal media (KBM-Gold) supplemented with growth kit (2 ml of bovine pituitary extract, 0.5 ml of insulin, transferrin, hydrocortisone, GA-1000 and r-human epidermal growth factor, and 0.25 ml of epinephrine, Lonza). Cells were incubated at 37° C in a 5% CO_2 atmosphere.

2. Asiaticoside treatment method

Asiaticoside (molecular weight=959.12) was purchased from Xi'an Bosheng Biomedical Technology (Xi'an, Shaanxi, China). To dissolve the water-insoluble asiaticoside, dimethyl sulfoxide (DMSO; Sigma-Aldrich Corporation, St. Louis, MO, USA) was used to prepare a stock solution of 200 mM asiaticoside for in vitro assays. The stock solution was diluted with serum free media without growth factors to concentrations of 0, 62.5, 125, 250, 500, and 1000 µM asiaticoside and cells were treated with equal volumes at each concentration. The same amount of DMSO was used to make various concentrations of asiaticoside using the stock solution and to avoid the effect of DMSO on skin cells behaviors.

3. Cell viability assay

The cytotoxicity of asiaticoside was evaluated using the 3-(4,5-dimethylthiazol-2-yl)-2,5-diphenyltetrazolium bromide (MTT) assay. The aHDFs were plated at a density of $1X10^5$ cells/ well in 48-well plates and aNHEKs were plated at $1X10^5$ cells/ well in 24-well plates. Cells were incubated for 24 h and treated with various concentrations of asiaticoside (62.5 µM to 1 mM) as described above. After 24 h of asiaticoside treatment, cells were incubated with 0.5 mg/ml of 3-(4,5-dimethylthiazol-2-yl)-2,5-diphenyltetrazolium bromide (Amresco, Inc., Solon, OH, USA) for

4 h in the dark. The formazan salts formed were dissolved in DMSO and the optical density was measured at 570 nm.

4. Cell migration assay

A wound closure seeding model was constructed using silicon culture inserts (Ibidi, LLC, Munchen, Germany) with two individual wells for cell seeding. Each insert was placed in a culture dish, and $8X10^3$ cells of aHDF or $2X10^4$ cells of aNHEK were plated in each well and grown to form a confluent and homogeneous layer. Twenty-four hours after cell seeding, the culture insert was removed and a cell-free area, the "wound" made by the culture insert, could be observed. The wound was approximately 500 μm wide. The cells were treated with 10 μg/ml of mitomycin C in serum free media without growth factors for 2 hr to suppress cell proliferation. Healing of the wound by migrating cells after asiaticoside treatment was observed over time by light microscopy (IX-70, Olympus, Japan) and analyzed using Image J software (NIH, USA). Schematic of cell migration assay is described in Figure 3.

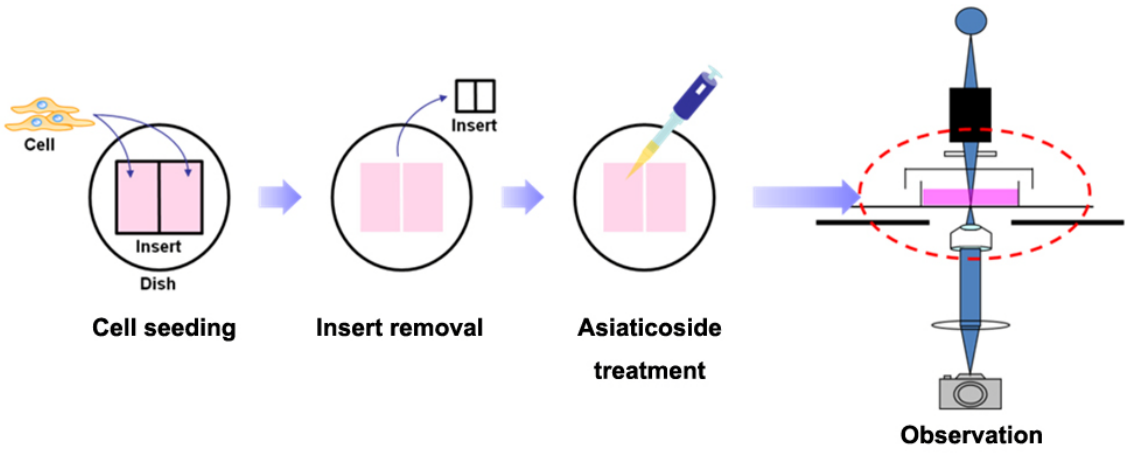

Figure 3. Schematic of cell migration assay. For wound closure seeding model, inserts with two wells were placed on 35∅ culture dish and cells were plated. After incubation, inserts were detached and asiaticoside was treated to the cells. Migration of cells was observed by optical microscope at given times.

5. Cell attachment assay

A. MTT assay

Cell attachment was determined at 4 to 6 hr after seeding, depending on the cell type, using the MTT assay. Briefly, fibroblasts were seeded at an initial density of $5X10^4$ cells/ well in 24-well plates with asiaticoside co-treatment and incubated for 4 hr in a CO_2 atmosphere. Keratinocytes were plated at the initial density of $5X10^4$ cells/ well in 48-well plates and treated as described above. Unattached cells were removed by gentle washing with phosphate buffered saline (PBS) and cell numbers attached were determined by MTT assay as described above.

B. Fluorescent staining

For cell morphometric analysis, cells were plated at the initial density of $5X10^4$ cells/ well in 24-well plates with asiaticoside co-treatment and incubated for 4-6 hr in a CO_2 atmosphere as described above. Cells were then fixed with ice-cold 70% ethanol for 30 min. Actin cytoskeleton was visualized by staining with Alexa (488)-conjugated phalloidin (1 U/sample, Invitrogen, Carlsbad, CA, USA) and cell nuclei were counterstained with propidium iodide (Sigma-Aldrich Corporation, Steinheim, Germany). Six random pictures were taken using an IX-70 microscope equipped with a DP-71 digital camera (Olympus). Areas with 30 cells attached were measured for each group using Image J software.

C. Adhesion molecule observation

Immunofluorescent staining of vinculin was performed to visualize focal adhesions. After 4 h of incubation after asiaticoside treatment, vinculin for focal adhesions and nucleus were visualized by immunostaining. Each step for immunostaining was as following. Cells were fixed with 3.7% paraformaldehyde (sigma) for 15 min at room temperature and were gently washed twice with PBS. Cells were permeabilized with 0.25% Triton X-100 in PBS for 5 min at room temperature and rinsed 3 times with PBS. Cells were blocked with 1% bovine serum albumin (BSA, sigma) in PBS with 0.1% tween20 for 30 minutes at room temperature and incubated with anti-vinculin primary antibody (1:60 dilution, SantaCruz Biotechnology, USA) overnight at 4℃. Cells were then washed three times with PBS for 5 min on the shaker. In dark, they were treated with Alexa-488-conjugated secondary antibody (1:100 dilution, SantaCruz) for vinculin staining and hoechst 33258 (1:1000 dilution) for nucleus staining for 30 min at room temperature. The cells were washed with PBS twice and observed with a fluorescent microscope.

6. Cell proliferation assay

For cell proliferation assay, cells were incubated for 1, 3 and 5 days after asiaticoside treatment. Cell numbers were determined by MTT assay for aHDFs and a 5-bromo-2'-deoxyuridine (BrdU) incorporation assay (Roche Applied Science, Basel, Switzerland) for aNHEKs.

A. MTT assay

To assess proliferation, aHDFs were plated at an initial density of $1X10^4$ cells/ well in 48-well plates and asiaticoside was treated. After incubation for 1, 3 and 5 days, cell numbers were determined by MTT assay for aHDFs as described above.

B. BrdU assay

Cells were plated at a density of $1X10^4$ cells/ well in 48-well plates and asiaticoside was treated. After incubation for 1, 3 and 5 days, cell numbers were determined by BrdU assay. For the BrdU incorporation assay, a BrdU-labeling solution was added to cells at given times and cells were returned to incubation for 2 h at 37°C. Labeling medium was then removed and the cells were incubated with fixation solution for 30 min at room temperature. The substrate solution was added and absorbance was measured at 370 nm with a 492 nm reference using an automatic microplate reader (Spectra Max 340, Molecular Devices, Inc., Sunnyvale, CA, USA).

7. Fabrication of 3D PLGA mesh

PLGA polymer (lactide/glycolide = 75/25) was purchased from Lakeshore Biomaterials (Birmingham, USA). PLGA was dissolved in a 1:4 mixture of dimethylformamide (DMF, Duksan Pure Chemicals co., Ltd., Ansan, Republic of Korea) and tetrahydrofuran (THF, Duksan Pure Chemicals co., Ltd.) at a concentration of 20% (w/v), and the mixture solvent was highly volatile.

The polymer solution was then loaded into a syringe with 21 gauge metal needle tip. The needle tip was connected to 20 kV of a high-voltage source and a metal drum collector was served as the ground for the electrical charges. The distance between the needle tip and the drum collector was 10 cm, and the polymer solution was ejected at 2 mL/h. For the deposition of ice crystals on the collector surface, the drum was loaded with dry ice which gives extremely low temperatures (-78.5°C) to the drum surface. Electrospun scaffold fabricated at room temperature without dry ice was manufactured for comparison. Environmental humidity was maintained at

50% approximately using a humidifier in both conditions. After fabrication, the meshes containing ice crystals were lyophilized to maintain porous structure. Schematic of low temperature electrospinning is described in Figure 4.

The surface and the cross-sectional morphology were observed with scanning electron microscope (SEM, S-4700, Hitachi, Tokyo, Japan). The porous meshes were coated with Pt by sputtering for 180 s before SEM observation.

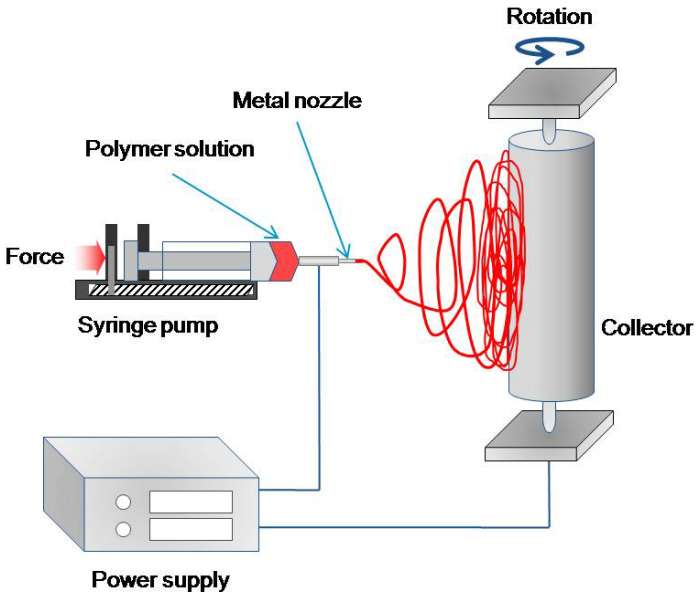

Figure 4. Schematic of low temperature electrospinning. Polymer solution was loaded into a syringe and metal needle tip was connected. Voltage source was connected to the connector between the syringe and the metal nozzle. Metal collector was filled with dry ice and grounded. High voltage was applied to fabricate polymer mesh and the fibers are collected on the rotating collector. The fabricated 3D meshes were freeze-dried.

8. Asiaticoside-containing 3D PLGA mesh

A. Fabrication of asiaticoside-containing 3D PLGA mesh

3D PLGA mesh was electrospun from 20% (w/v) solution in THF/DMF (4/1) and asiaticoside 0, 5 and 10wt% of PLGA weight was dissolved with PLGA for the fabrication of asiaticoside-containing 3D PLGA mesh. As described above, the metal collector was loaded with dry ice and environmental humidity was maintained at about 50% using a humidifier. For the optimal electrospinnng condition, applied voltage was controlled. Finally, the polymer solution-loaded syringe was connected with 21 gauge metal needle and 13.5 kV of a high-voltage was applied. Fibers fabricated were deposited on the grounded metal collector. The distance between the needle tip and collector was 10 cm, and the polymer solution was ejected at 2 mL/h. Manufactured meshes were freeze-dried and the surface morphology was observed with a SEM (Hitachi). The meshes were coated with Pt by sputtering for 180 s before SEM observation.

B. Release pattern of asiaticoside-containing 3D PLGA mesh

For the observation of release pattern of asiaticoside-containing 3D PLGA mesh, 10% ethanol in distilled water was used as release medium. Small amount of ethanol was used because of low solubility of asiaticoside to water.

Three pieces of asiaticoside-containing 3D PLGA mesh were placed in a vial filled with 3 ml of release medium. Drug release studies were carried out at 35 °C in thermostatic shaking incubator. Total volume of release medium was taken and the same volume of fresh medium was replaced. Optical density of the taken medium was observed using UV spectrophotometer at a wavelength of 409 nm. In the assessment of drug release behavior, the accumulated amount of released drug was calculated from standard curve data.

C. Cytotoxicity of asiaticoside-containing 3D PLGA mesh

The cytotoxicity of asiaticoside-containing 3D PLGA mesh was evaluated using picogreen assay (Quant-iT™ PicoGreen ® dsDNA Reagent and Kits, Invitrogen). The aHDFs were plated at a density of $2X10^5$ cells/ well on the sample respectively. Serum free media without growth kit was used to plate cells. Cells were incubated for 5 d. After incubation, samples were washed gently with PBS and 500 μl of 0.1% triton X-100 in TE buffer(10 mM Tris-HCl, 1 mM EDTA, pH 7.5) was treated as a cell lysis buffer. For better lysis, samples were chopped and then freezed and thawed twice. Finally thawed samples were collected and centrifuged at 4°C, 12000 rpm for 10 minutes. Supernatant of the sample was collected and 100 μl of the supernatant

was reacted with 100 μl of picogreen reaction solution (2 μg/ml). The samples were excited at 480 nm and the fluorescence emission intensity was measured at 520 nm using a spectrofluorometer. (LS-50B, PerkinElmer, USA)

D. Attachment effect of asiaticoside-containing 3D PLGA mesh

Attachment of aHDFs on the asiaticoside-containing 3D PLGA mesh was evaluated using picogreen assay as described before. The aHDFs were plated at a density of $5X10^4$ cells/ sample using serum free media without growth kit, and cells were incubated for 4 h. Samples were then washed gently with PBS and 500 μl of 0.1% triton X-100 in TE buffer was treated for cell lysis. Freeze-thaw cell lysis method was used as described above. The samples were collected and centrifuged at 4°C, 12000 rpm for 10 minutes, and 100 μl of the supernatant was mixed with 100 μl of picogreen reaction solution. The samples were excited at 480 nm and the fluorescence emission intensity was measured at 520 nm using a spectrofluorometer.

E. Growth rate effect of asiaticoside-containing 3D PLGA mesh

Growth rate of aHDFs on the asiaticoside-containing 3D PLGA mesh was measured using picogreen assay. The aHDFs were plated at a density of $4X10^4$ cells/ sample using serum free media without growth kit, and cells were incubated for 1, 3 d. Samples were then washed gently with PBS and 500 μl of 0.1% triton X-100 in TE buffer was treated for cell lysis. Freeze-thaw cell lysis method was used as described above. The samples were collected and centrifuged at 4°C, 12000 rpm for 10 minutes, and 100 μl of the supernatant was mixed with 100 μl of picogreen reaction solution. The samples were excited at 480 nm and the fluorescence emission intensity was measured at 520 nm using a spectrofluorometer.

9. Statistical analysis

All results are expressed as mean ± standard deviation of mean and analyzed by Student t-test. Statistical significance was considered at $p<0.05$.

III. RESULTS

1. Cell viability assay

Before applying asiaticoside to skin cells for evaluation of its beneficial effect to wound healing, cellular toxicity was investigated using MTT assay in advance.

Figure 5 shows the cytotoxicity of asiaticoside evaluated by the 3-(4,5-dimethylthiazol-2-yl)-2,5-diphenyltetrazolium bromide (MTT) assay. DMSO treated group was used as a control group. In the cell viability assay, asiaticoside was not cytotoxic in aHDFs at any concentration from 61.5 to 1000 μM and in aNHEKs at concentrations from 61.5 to 500 μM. At 1000 μM, however, asiaticoside decreased the viability of aNHEKs.

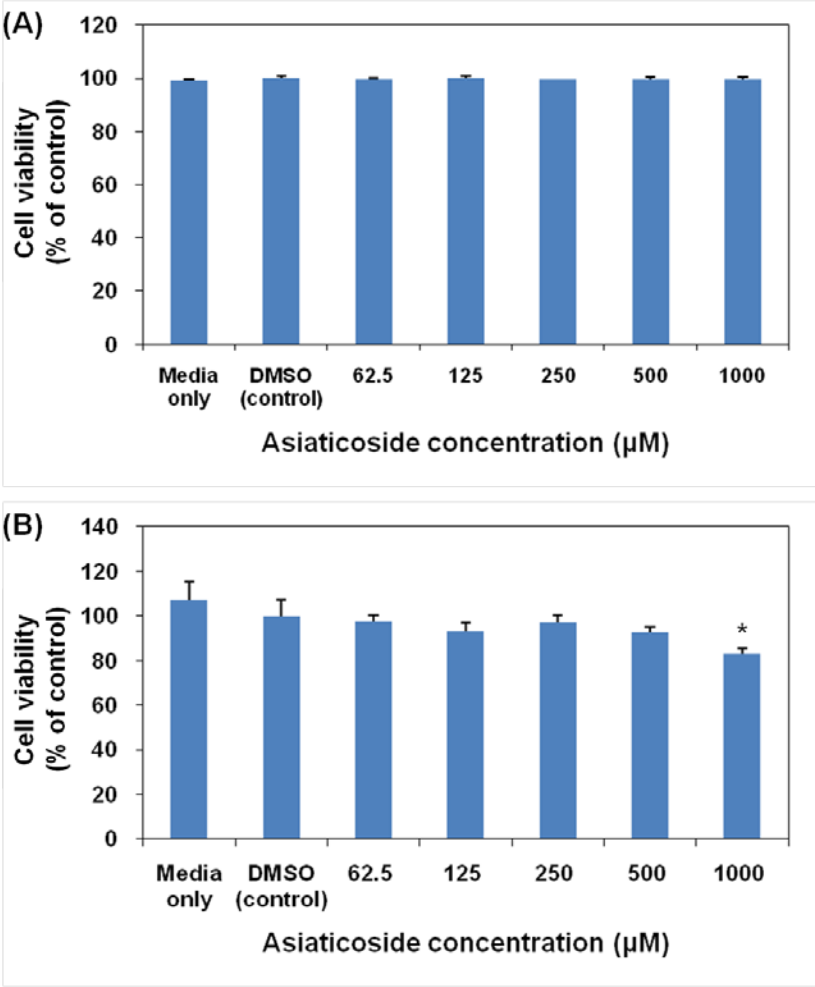

Figure 5. Effect of asiaticoside on the viability of aHDFs and aNHEKs was measured by MTT assay. (A) Asiaticoside did not show any cytotoxicity on aHDFs up to the concentration of 1 mM. (B) Asiaticoside showed cytotoxicity on aNHEK at a concentration of 1 mM only. *$p < 0.05$ compared with DMSO control group.

2. Cell migration assay

Based on the results of cell viability test, asiaticoside under 1 mM of concentration was treated to the skin cells for the rest of experiments.

Figure 6 shows the effects of asiaticoside on migration of normal human skin cells at every 24 h. The graphs in figure 6 indicate the repaired area by migrated cells compared with original wound size. Compared with a control group, asiaticoside-treated cells migrated faster, and the most effective concentration varied with cell type. In fibroblasts, asiaticoside at 250 μM increased migration rate most effectively and showed improvement on wound healing area compared with a control group (Figure 6 (A)). In keratinocytes, 500 μM of asiaticoside improved wound healing by about 30% as shown in covered area by migration of cells into the wound (Figure 6 (B)).

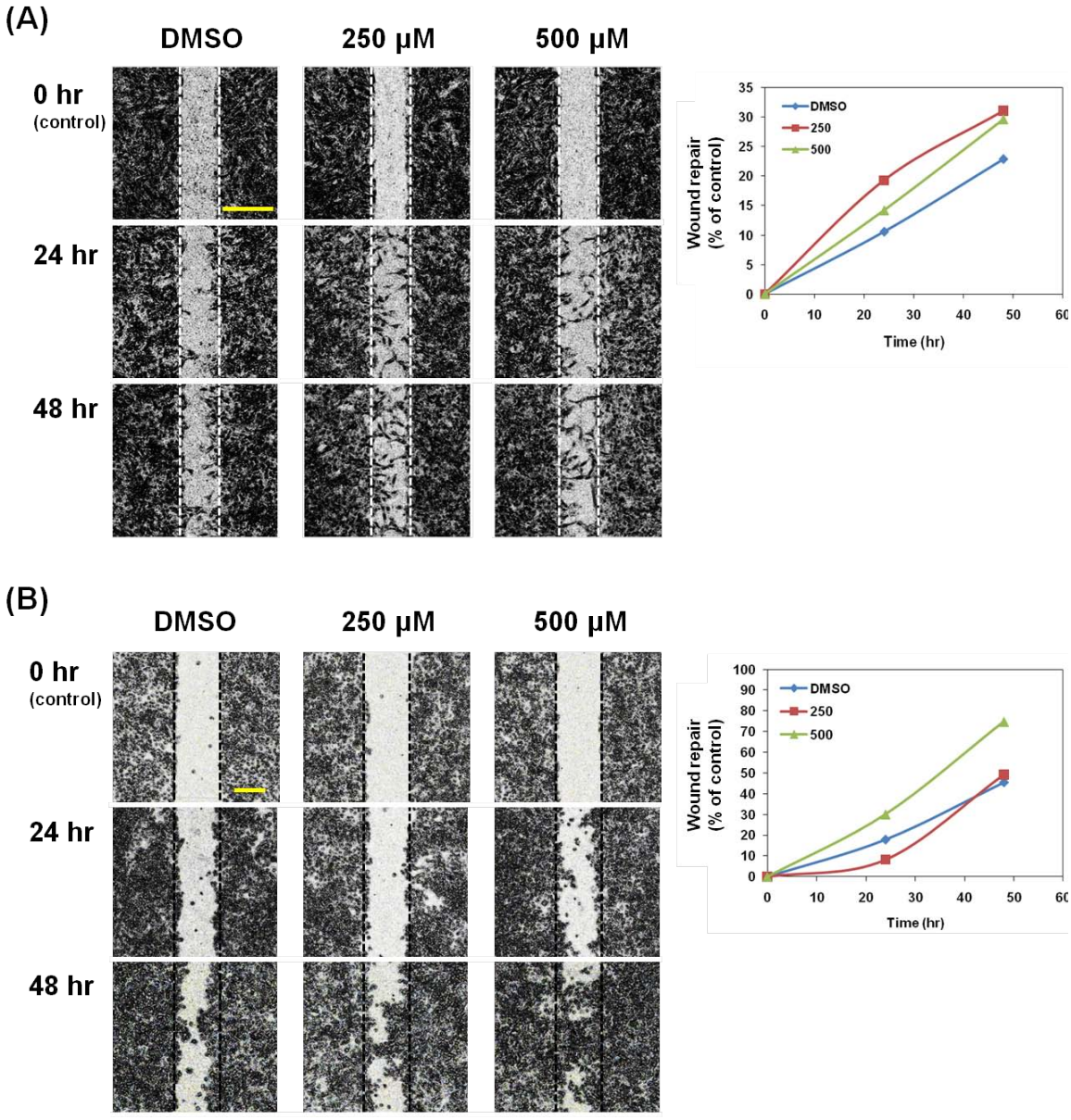

Figure 6. Effect of asiaticoside on the migration of aHDFs and aNHEKs were observed with optical microscope. Asiaticoside increases the migratory speed of (A) aHDFs and (B) aNHEKs compared with DMSO control group. Scale bar=400 μm.

3. Cell attachment assay

A. MTT assay & Fluorescent staining

To investigate the effect of asiaticoside on initial adhesion and spreading of skin cells, cells were treated with increasing concentrations of asiaticoside in serum-free media for 4-6 h. In Figure 7, (A) and (C) show the numbers of aHDFs and aNHEKs attached as investigated by MTT assays, and (B) and (D) show the cell attachment areas of aHDFs and aNHEKs, respectively, as observed by fluorescent staining. As shown in Figure 7 (A), asiaticoside treatment significantly enhanced the numbers of fibroblasts attached by approximately 40%. Figure 7 (C) indicates that the attached numbers of keratinocytes was increased by more than 10%. At 1000 μM asiaticoside, aNHEKs appeared to decrease in number, which may indicate cell type-specific cytotoxicity. Asiaticoside also increased the areas occupied by attached skin cells (Figure 7, (B) and (D)).

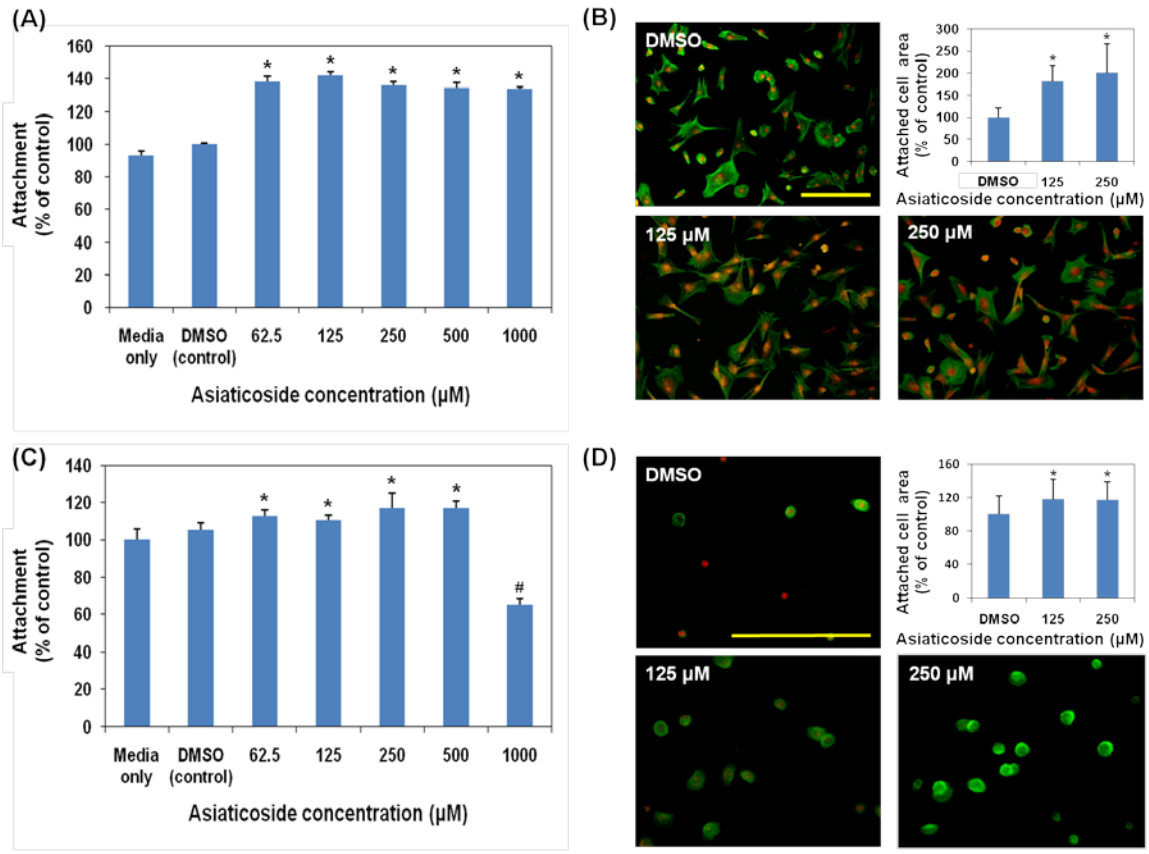

Figure 7. Effect of asiaticoside on the attachment of aHDFs and aNHEKs were investigated by MTT assay and fluorescent staining. (A) Attached cell number and (B) attached cell area of aHDFs were increased by asiaticoside treatment. (C) Attached cell number and (D) attached cell area of aNHEKs were increased by asiaticoside. * $p < 0.05$ compared with DMSO control. # $p < 0.05$ compared with cells treated with the other concentrations. Scale bar= 50 μm.

B. Adhesion molecule observation

Vinculin is a 116 kDa actin-binding protein that is associated with cell–cell and cell–extracellular matrix junctions.

After 4 h of incubation, focal adhesion formation was observed by anti-vinculin immunostaining. Immunofluorescence images of aHDFs stained for nucleus (blue) and vinculin (green) and merged images of nucleus and vinculin are shown in Figure 8. As shown in Figure 8, stronger vinculin signals in peripheral regions of cells as well as throughout the cellular extensions were observed in asiaticoside-treated cells compared with DMSO control group.

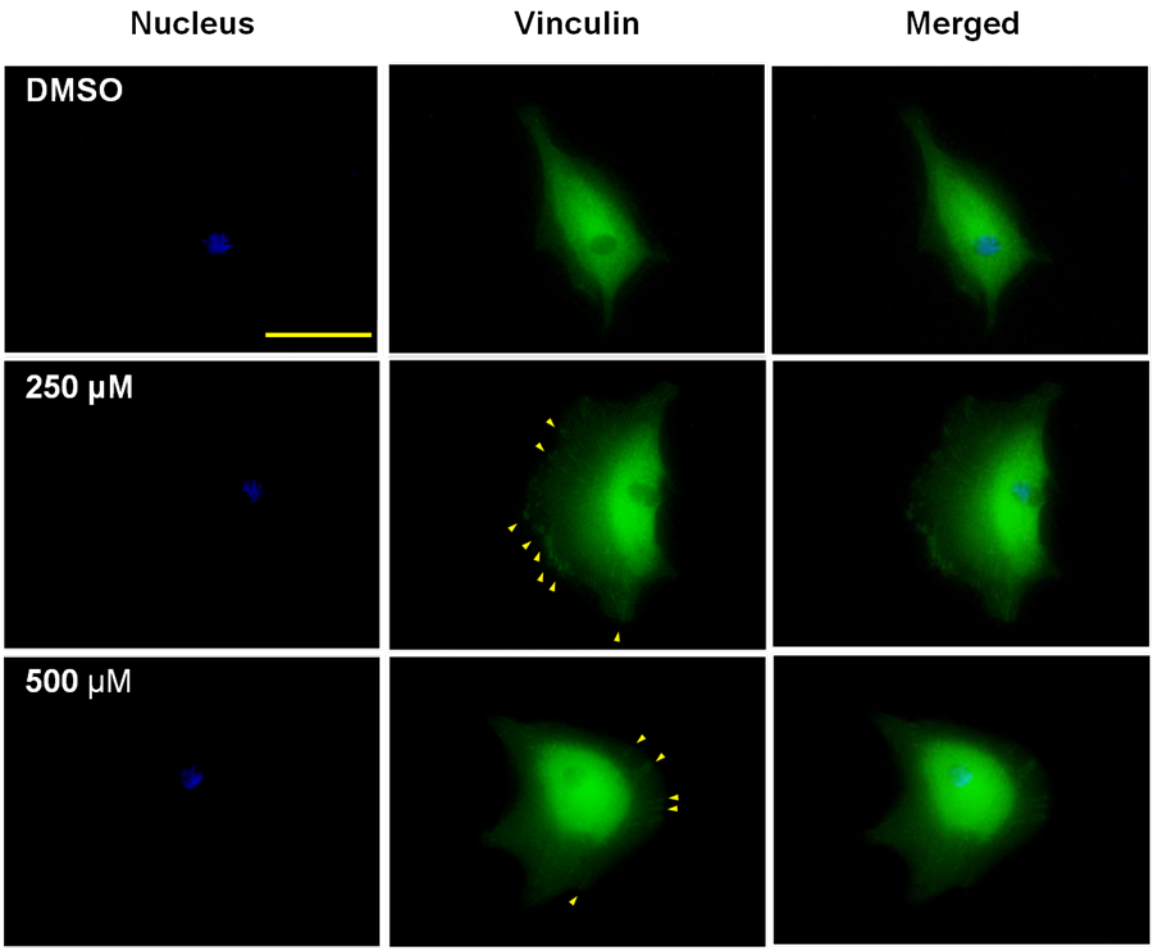

Figure 8. Effect of asiaticoside on the adhesion molecule expression of aHDFs was evaluated by immunofluorescent staining. Vinculin expression of aHDFs was increased by asiaticoside treatment compared with DMSO control group. Scale bar = 100 μm.

4. Cell proliferation assay

In a dose-dependent manner, asiaticoside promoted the growth of fibroblasts (Figure 9 (A)). At 62.5 μM asiaticoside, the cell number did not increase significantly compared with a control DMSO until the 3 d. cells treated with 62.5 μM of asiaticoside were increased significantly at 5 d in comparison with the control. However, at 125 μM and higher concentrations of asiaticoside the numbers of treated cells increased steadily from 1 to 5 d compared with the control group. In contrast, asiaticoside did not influence the growth rate of keratinocytes (Figure 9 (B)).

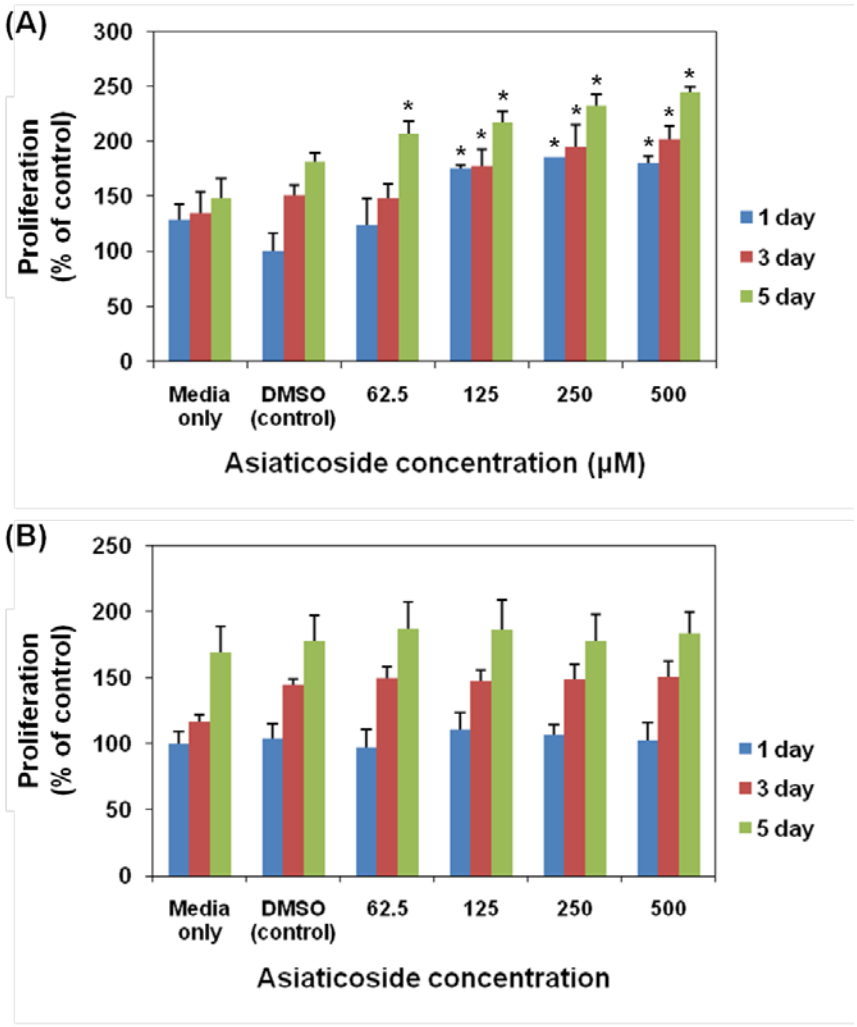

Figure 9. Effect of asiaticoside on the proliferation of aHDFs and aNHEKs were evaluated by MTT and BrdU assay respectively. (A) Asiaticoside increases the growth rate of aHDFs compared with DMSO control group. (B) The growth rate of aNHEKs was not affected by asiaticoside treatment. * $p < 0.05$ compared with DMSO control group.

5. Fabrication of 3D PLGA mesh

For the fabrication of PLGA mesh having porous 3D structured mesh, electrospinning method at low temperature was carried out. Electrospun scaffolds manufactured at room temperature were used as a control.

In Figure 10, the surface morphology and the cross-sectional morphology were observed with a SEM. According to the results, both of meshes has similar fiber diameter but meshes fabricated at low temperature showed more porous 3D structure than meshes fabricated at room temperature. Also, the results indicate that the fabrication of scaffolds having sufficient thickness to replace injured skin is possible by using low temperature electrospinning method.

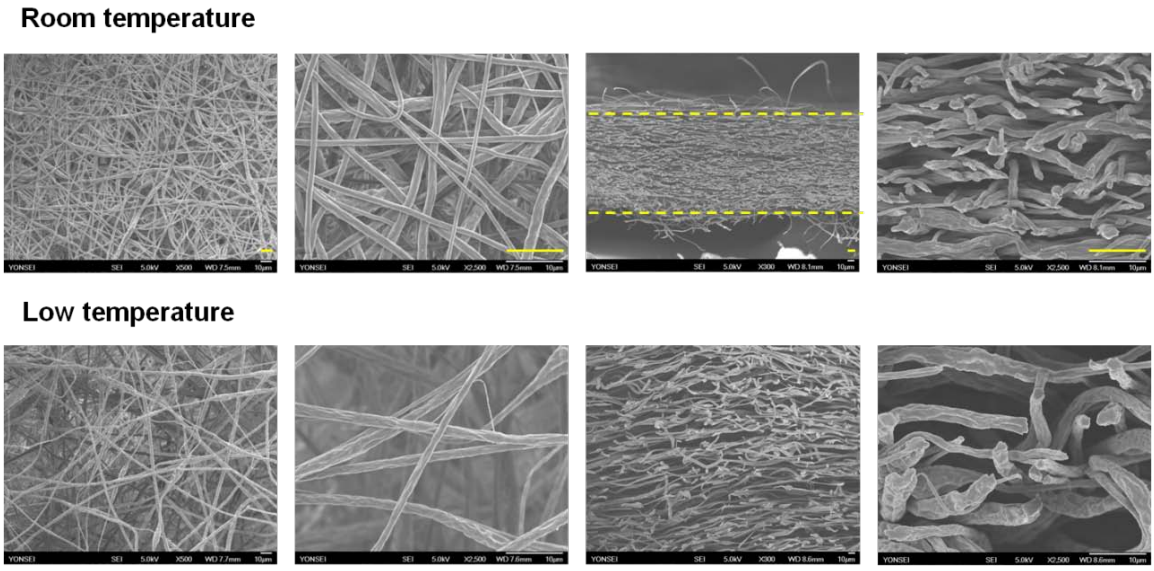

Figure 10. Morphology of PLGA mesh fabricated at room temperature and low temperature was observed with SEM. Surface (left side) and cross section (right side) of electrospun RT mesh. Dotted line indicates the edge of the RT mesh. Surface (left side) and cross section (right side) of electrospun LT mesh showed higher porosity than RT mesh. The edge of the RT mesh could not be outlined because of its thickness. Scale bar= 10 μm.

6. Asiaticoside-containing 3D PLGA mesh

A. Fabrication of asiaticoside-containing 3D PLGA mesh

Bioactive compounds have been applied to polymer scaffolds for tissue engineering to increase biocompatibility of the scaffolds and to help tissue regeneration. In this study, asiaticoside was chosen as a bioactive compound.

Three-dimensional PLGA meshes containing 0, 5, 10, 20 wt% asiaticoside were fabricated, but the mesh with 20 wt% asiaticoside was too weak to keep in shape. Surface morphology of fabricated 3D PLGA mesh containing asiaticoside was observed with a SEM. On the surface of the fiber, asiaticoside educed after lyophilization from the surface of the fiber was observed. Average fiber diameters of the mesh were similar regardless of asiaticoside contents (Figure 11).

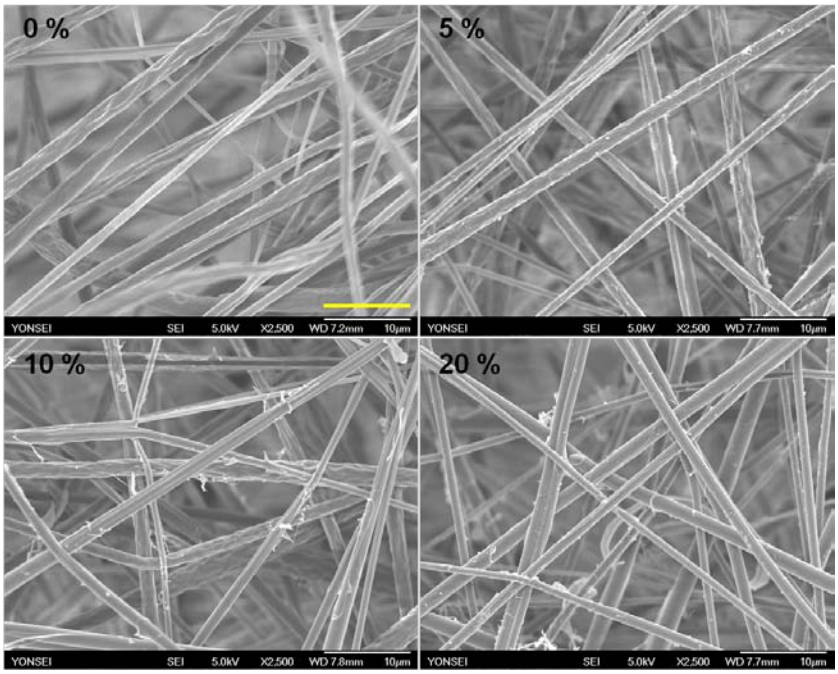

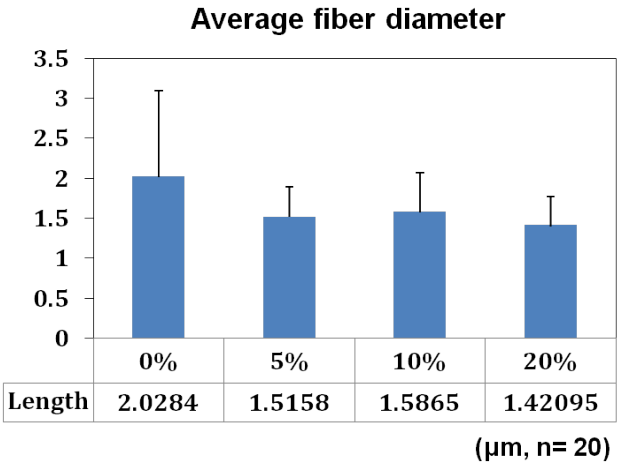

Figure 11. Morphology of fabricated 3D PLGA mesh containing asiaticoside was observed with SEM and the average fiber diameters of each mesh was analyzed using Image J software. Average fiber diameters of the meshes were similar regardless of asiaticoside contents. Scale bar= 10 μm.

B. Release pattern of asiaticoside-containing 3D PLGA mesh

For the observation of release pattern of asiaticoside-containing 3D PLGA mesh, 10% methanol in distilled water was used as release medium and 700 μl of the solution was taken to measure spectrum at a given time (1, 3 and 6 h, 1, 3 and 5 d).

Early and final release pattern of PLGA mesh containing asiaticoside was observed (Figure 12). Most of asiaticoside incorporated in PLGA mesh was released rapidly during initial 6 hr as shown in Figure 12(A). Dashed line indicates the concentration calculated based on the actual amount of asiaticoside loaded in each mesh. Approximately 77% of the actual asiaticoside amount was released from 5% asiaticoside-containing mesh and about 74% of the actual asiaticoside amount was released from 10% asiaticoside-containing mesh. Total release pattern of asiaticoside-containing 3D PLGA mesh up to 5 days is shown in Figure 12(B). According to the results, 82% of the actual asiaticoside amount was released from the meshes containing 5% asiaticoside and 97% of the actual asiaticoside amount was released from the meshes containing 10% asiaticoside, approximately.

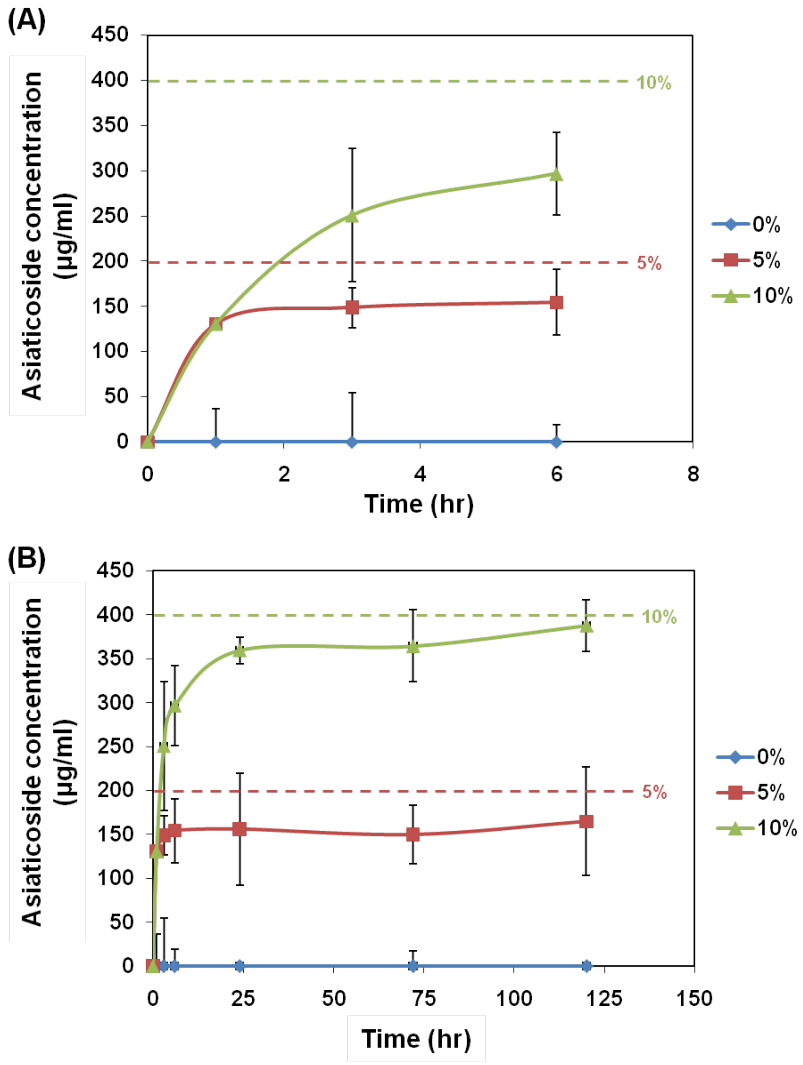

Figure 12. Release pattern of asiaticoside from asiaticoside-containing 3D PLGA mesh was evaluated with spectrophotometer. (A) Initial release pattern of 3D PLGA mesh containing asiaticoside up to 6 hr. (B) Total release pattern of of 3D PLGA mesh containing asiaticoside.

C. Cytotoxicity of asiaticoside-containing 3D PLGA mesh

Cell viability on the asiaticoside-containing 3D PLGA mesh was evaluated before applying the mesh to skin cells.

The viability of aHDFs on an asiaticoside-containing 3D PLGA mesh was evaluated using picogreen assay and it showed asiaticoside incorporated in the mesh did not have any cytotoxicity until 20%. (Figure 13) However, meshes containing asiaticoside 20 wt% of PLGA showed weak physical properties to keep in shape as mentioned before, and therefore following experiments were carried out using 0, 5 and 10 wt% asiaticoside-containing PLGA mesh.

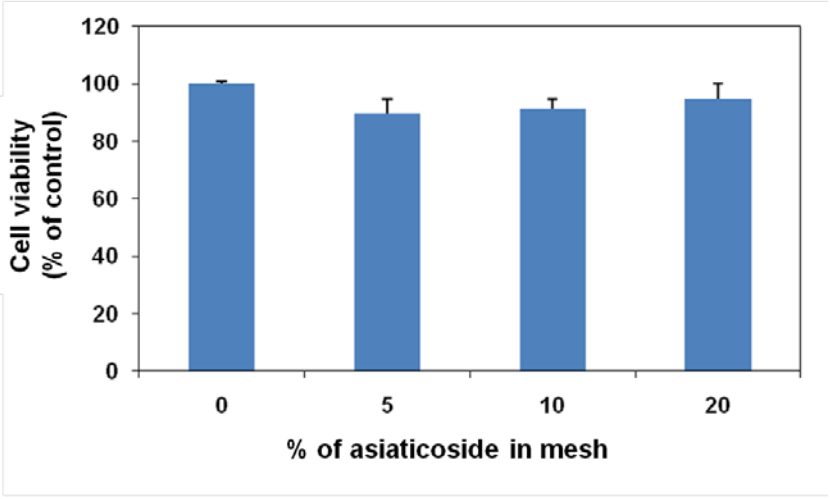

Figure 13. Cytotoxicity of asiaticoside-containing 3D PLGA mesh against aHDFs was measured by picogreen assay.

D. Attachment effect of asiaticoside-containing 3D PLGA mesh on aHDFs

In Figure 14, the attachment of aHDFs on the asiaticoside-containing 3D PLGA mesh was evaluated using picogreen assay. The attached cell number on the mesh containing asiaticoside was compared with the number of cells attached on the control PLGA mesh and the results are shown as % of control. At a low concentration of 5%, asiaticoside in the mesh enhanced the initial adhesion of aHDFs on the fabricated mesh. However, it did not affect the attachment of aHDFs on the mesh at a comparably high concentration of 10%.

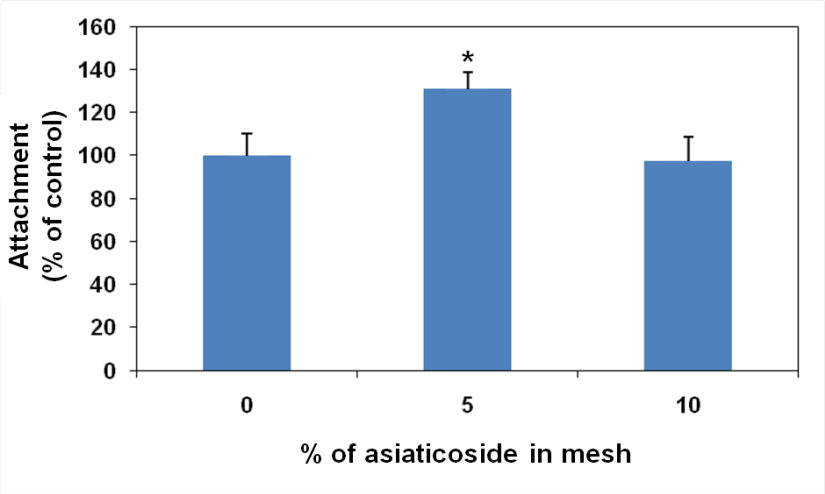

Figure 14. Effect of asiaticoside-containing 3D PLGA mesh on the attachment of aHDFs was measured by picogreen assay. * $p < 0.05$ compared with 0% control group.

E. Growth rate effect of asiaticoside-containing 3D PLGA mesh

The growth rate of aHDFs on the asiaticoside-containing 3D PLGA mesh was evaluated using picogreen assay (Figure 15). The number of cells proliferated on the mesh containing asiaticoside was compared with the cell number proliferated on the control PLGA mesh, and the results are shown as % of control. At a concentration of 5%, the mesh containing asiaticoside enhanced the growth rate of aHDFs on the fabricated mesh.

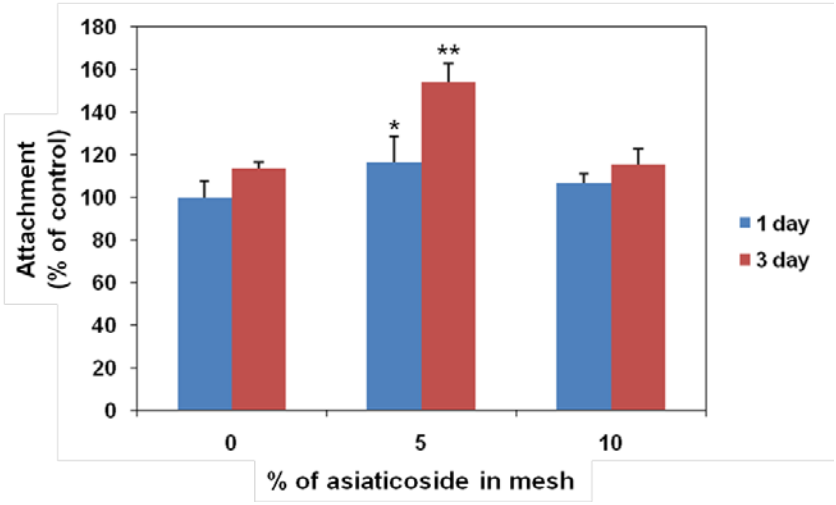

Figure 15. Effect of asiaticoside-containing 3D PLGA mesh on the proliferation of aHDFs was measured by picogreen assay. * $p < 0.05$ compared with 0% control group. ** $p < 0.01$ compared with 0% control group.

IV. DISCUSSION

In hypertrophic scars and keloids, asiaticoside may increase the expression of matrix metalloproteinase-1 (MMP-1), and this may induce an intermediate state of cell adhesiveness (cellular "de-adhesiveness") that may be involved in tissue adaptation and repair[15-17]. Asiaticoside may also down-regulate the expression of tissue inhibitor of metalloprotease-1 (TIMP-1). These findings suggest that asiaticoside-induced cell migration might contribute to an adaptive morphogenic process such as healing.

In this study, it was revealed that asiaticoside enhances cellular migration, initial adhesion and proliferation for the skin cells except the growth rate of keratinocytes. Winter et al. has suggested that movement of epidermal cells on the surface of the wound influences epidermal repair in cutaneous wound healing[18]. New tissue formation during wound repair is characterized by migration and proliferation of different cell types including keratinocytes and fibroblasts. It is therefore plausible that asiaticoside may promote tissue repair by increasing skin cell migration rates.

Cell adhesion occurs in three stages, i.e., attachment, spreading, and the formation of focal adhesions and stress fibers[19,20]. The spreading of cells may be involved in adhesion stability. In this study, we observed the enhanced numbers of skin cells attached, the enlarged adhesion area and the strong expression of vinculin, one of the adhesion molecules, after asiaticoside treatment. Therefore, our findings indicate that asiaticoside may facilitate and stabilize skin cell adhesion.

Asiaticoside is known to induce a dual specificity protein phosphatase (DUSP) and dual specificity phosphatase 3 (DUSP3) that negatively regulate the mitogen-activated protein (MAP) kinase superfamily and associated with cellular proliferation and differentiation, in normal human dermal fibroblasts[21]. On the other hand, asiaticoside has been reported to have an antiproliferative effect on hypertrophic and keloid keratinocytes[22]. In this study, asiaticoside enhanced proliferation in normal human dermal fibroblasts and did not affect the growth rate of normal human epidermal keratinocytes.

Several kinds of methods such as autograft, homograft and heterograft are introduced for the regeneration of skin tissue impaired by burn, cutaneous wound and skin diseases. These are valuable methods to substitute injured tissue but still have limitations due to the short supply and high prices. Therefore, polymer scaffolds with high biocompatibility could be promising materials for tissue repair because of its reasonable price and easy fabrication.

PLGA is a type of biodegragable polymer and is approved its safety by FDA. It has been used for a number of years for a wide range of clinical applications such as resorbable sutures and stents[23,24]. Dermal replacements of PLGA were introduced by Blackwood et al. but the scaffold did not meet the sufficient thickness and several layers of the scaffolds were placed together[25].

It is obvious that the characteristics of scaffold such as pore size and fiber structure could regulate cellular proliferation, organization and finally subsequent tissue morphogenesis. High porosity structures could improve the fluid exchange, infiltration and migration of cells. Recently, the researchers have been developed that the high porosity scaffolds using electrospinning by mixing with other materials and controlling of the process parameters such as solvent system and collector design[26,27]. Simonet et al. had been investigated a simple method to increase porosity of mesh by ice crystals using dry ice[28]. The ice crystals were formed at low-temperature with high humidity. In this study, low temperature electrospinning method was introduced to fabricate dermal replacements and the electrospun meshes showed porous and thick structures enough to substitute skin layer.

The initial cell adhesion and proliferation activities would be especially important in the use of artificial skin preparations such as wound dressings and scaffolds for tissue engineering. In the case of a full-thickness skin wound with loss of both of epidermis and dermis, an artificial skin can be used to stand in for both skin layers and promote cutaneous wound repair. Currently, bioactive compounds may be introduced into artificial skins to promote healing. Merrell *et al.* incorporated curcumin isolated from the root of *Curcumin longa L* into poly(caprolactone) as a diabetic wound dressing with anti-oxidant and anti-inflammatory properties[29]. Film- and foam-like structures of N-carboxybutylchitosan and of agarose impregnated with quercetin and thymol show properties compatible with use in wound dressings[30]. Asiaticoside also has been loaded in alginate films[31] and electrospun gelatin[32] and cellulose acetate fiber mats[33] as a possible use for topical/transdermal or wound dressing patches. Our findings about cell adhesion and proliferation suggest that if asiaticoside is incorporated into 3D PLGA mesh for substituting damaged dermis, dermal fibroblasts around the substitute would adhere to and proliferate into the artificial dermis and therefore the wounds could be repaired more rapidly and securely.

V. CONCLUSION

Migration, adhesion and proliferation are vital skin cell behaviors in wound repair. In this study, asiaticoside increased the migration rates and initial attachment of skin cells and promoted normal human dermal fibroblast proliferation. Skin cell behaviors such as spreading and migration are major determinants of the wound closure rate. The biological activities of asiaticoside support its use as a promoter of wound healing and potentially, as a bioactive component of an artificial skin.

REFERENCES

1. Braun-falco O, Plewig G, Wolff HH, Burgdorf WHC. Dermatology. 2nd ed. Berlin Heidelberg New York: Springer; 2000.
2. Zouboulis CC. Human skin: An independent peripheral endocrine organ. Horm Res Paediatr 2000;54:230-42.
3. Singer AJ, Clark R. Cutaneous wound healing. N Engl J Med 1999;341:738-46.
4. Serarslan G, Güler H, Karazincir S. The relationship between nail-and distal phalangeal bone involvement severity in patients with psoriasis. Clin Rheumatol 2007;26:1245-7.
5. Gurtner GC, Werner S, Barrandon Y, Longaker MT. Wound repair regen 2008;45:314-21.
6. Wong T, McGrath J, Navsaria H. The role of fibroblasts in tissue engineering and regeneration. Br J Dermatol 2007;156:1149-55.
7. Gupta A, Kumar R, Pal K, Banerjee PK, Sawhney RC. A preclinical study of the effects of seabuckthorn (hippophae rhamnoides L.) leaf extract on cutaneous wound healing in albino rats. Int J Low Extrem Wounds 2005;4:88-92.
8. Phan TT, Wang L, See P, Grayer RJ, Chan SJ, Lee ST. Phenolic compounds of chromolaena odorata protect cultured skin cells from oxidative damage: Implication for cutaneous wound healing. Biol Pharm Bull 2001;24:1373-9.
9. Kim SK, Mendis E. Bioactive compounds from marine processing byproducts–a review. Food Res Int 2006;39:383-93.
10. Guo JS, Cheng CL, Koo M. Inhibitory effects of centella asiatica water extract and asiaticoside on inducible nitric oxide synthase during gastric ulcer healing in rats. Planta Med 2004;70:1150-4.
11. Boiteau P, Ratsimamanga AR. Asiaticoside extracted from Centella asiatica and its therapeutic uses in cicatrization of experimental and refractory wounds (leprosy, cutaneous tuberculosis and lupus). Therapie 1956;11(1):125-49.
12. Shukla A, Rasik A, Jain G, Shankar R, Kulshrestha D, Dhawan B. In vitro and in vivo wound healing activity of asiaticoside isolated from centella asiatica. J Ethnopharmacol 1999;65:1-11.
13. Ju-lin X, Shao-hai Q, Tian-zeng L, Bin H, Jing-ming T, Ying-bin X, et al. Effect of asiaticoside on hypertrophic scar in the rabbit ear model, J Cutan Pathol 2009;36:234-9.
14. Tang B, Zhu B, Liang Y, Bi L, Hu Z, Chen B, et al. Asiaticoside suppresses collagen expression and TGF-β/Smad signaling through inducing Smad7 and inhibiting TGF-βRI and TGF-βRII in keloid fibroblasts. Arch Dermatol Res 2011;303:563-72.
15. El-Hefnawi H. Treatment of keloid with asiaticoside. Dermatologica 1962;125:387-92.

16. Lu X, Xu M, Shen G. The expression of TGF-beta~ 1 and MMP-1 in human pathological scar tissues. Jiangsu Med J 2005;31:901.
17. Zhang T, Rong XG, Yang RH, Li TZ, Xu YB. Effect of asiaticoside on the expression of transforming growth factor-beta mRNA and matrix metalloproteinases in hypertrophic scars. Nan Fang Yi Ke Da Xue Xue Bao 2006;26:67-70.
18. Winter G. Movement of epidermal cells over the wound surface. Adv Biol Skin 1964;5:113-27.
19. Murphy-Ullrich JE. The de-adhesive activity of matricellular proteins: Is intermediate cell adhesion an adaptive state?, J Clin Invest 2001;107:785-90.
20. Min BM, Lee G, Kim SH, Nam YS, Lee TS, Park WH. Electrospinning of silk fibroin nanofibers and its effect on the adhesion and spreading of normal human keratinocytes and fibroblasts in vitro. Biomaterials 2004;25:1289-97.
21. Lu L, Ying K, Wei S, Fang Y, Liu Y, Lin H, et al. Asiaticoside induction for cell-cycle progression, proliferation and collagen synthesis in human dermal fibroblasts. Int J Dermatol 2004;43:801-7.
22. Sampson J, Raman A, Karlsen G, Navsaria H, Leigh I. In vitro keratinocyte antiproliferant effect of centella asiatica extract and triterpenoid saponins. Phytomedicine 2001;8:230-5.
23. Jain RA. The manufacturing techniques of various drug loaded biodegradable poly(lactide-co-glycolide) (PLGA) devices. Biomaterials 2000;21(23):2475-90.
24. Lu JM, Wang X, Marin-Muller C, Wang H, Lin PH, Yao Q, et al. Current advances in research and clinical applications of PLGA-based nanotechnology. Expert Rev Mol Diagn 2009;9(4):325–41.
25. Blackwood KA, McKean R, Canton I, Freeman CO, Franklin KL, Cole D, et al. Development of biodegradable electrospun scaffolds for dermal replacement. Biomaterials 2008;29:3091–104
26. Yoon JJ, Park TG. Degradation behaviors of biodegradable macroporous scaffolds prepared by gas foaming of effervescent salts. J Biomed Mater Res B: Appl Biomat 2001;55:401-8.
27. Miller DC, Thapa A, Haberstroh KM, et al. Endothelial and vascular smooth muscle cell function on poly(lactic-co-glycolic acid) with nano structured surface features. Biomaterials 2004;25:53-61
28. Simonet M, Schneider OD, Neuenschwander P, et al. Ultraporous 3D polymer meshes by low-temperature electrospinning: using of ice crystals as a removable void template. Polym Eng Sci 2007;47:2020-6.

29. Merrell JG, McLaughlin SW, Tie L, Laurencin CT, Chen AF, Nair LS. Curcumin-loaded poly (ε-caprolactone) nanofibres: Diabetic wound dressing with anti-oxidant and anti-inflammatory properties. Clin Exp Pharmacol Physiol 2009;36:1149-56.
30. Dias A, Braga M, Seabra I, Ferreira P, Gil M, de Sousa H. Development of natural-based wound dressings impregnated with bioactive compounds and using supercritical carbon dioxide. Int J Pharm 2011;408:9-19.
31. Sikareepaisan P, Ruktanonchai U, Supaphol P. Preparation and characterization of asiaticoside-loaded alginate films and their potential for use as effectual wound dressings. Carbohydr Polym 2011;83:1457–69.
32. Sikareepaisan P, Suksamrarn A, Supaphol P. Electrospun gelatin fiber mats containing a herbal—Centella asiatica—extract and release characteristic of asiaticoside. Nanotechnology 2008;19:015102.
33. Suwantong O, Ruktanonchai U, Supaphol P. Electrospun cellulose acetate fiber mats containing asiaticoside or Centella asiatica crude extract and the release characteristics of asiaticoside. Polymer 2008;49:4239–47

ABSTRACT (IN KOREAN)

아시아티코사이드의 상처 치유 효과와 3 차원 생분해성 고분자 메쉬로의 적용

<지도교수 박종철>

연세대학교 대학원 의과학과

이 정 현

피부에 상처가 발생하면 일련의 단계에 따라 세포들이 고유의 역할을 하여 창상 치유가 이루어진다. 그 중 표피 케라틴세포와 진피 섬유아세포는 재상피화를 통한 창상부위의 보호와 상처로 인해 손실된 조직에서 육아조직 및 진피층을 형성하는 등 중요한 역할을 한다. 병풀은 오랜 과거로부터 아시아 여러 국가에서 다양한 피부질환을 치료하기 위한 약재로 사용되어 왔다. 병풀의 유효성분 중 특히 아시아티코사이드는 항생물질로 분류되는 트리테르펜 글리코사이드 계열 물질로써, 항염증 작용을 하며 켈로이드 및 비후성 반흔 치유에 효과가 우수한 것으로 알려져 있다. 그러나 아시아티코사이드가 정상 인간 피부세포에 미치는 영향은 명확히 밝혀져 있지 않다. 이에 따라 본 실험에서는 아시아티코사이드가 사람의 정상 피부 유래세포에 미치는 영향을 확인하기 위한 세포 실험을 진행하였다. 그 결과, 아시아티코사이드가 두 피부유래세포의 이동과 초기 부착 및 세포확산을 촉진시킨다는 것을 확인하였다. 또한 아시아티코사이드가 진피 섬유 아세포의 증식을 향상시킨다는 사실을 확인하였다.

표피와 진피가 모두 손실된 광범위한 피부 상처 치유를 위해서는 3 차원 구조의 진피대체용 지지체가 사용되는데 천연고분자로 제작된 지지체의 경우 좋은 임상적 결과를 얻고 있으나, 높은 원가와 공정의 어려움으로 상용화에 어려움이 있다. 한편 합성고분자로 제작된 지지체의 경우 제작 비용이 비교적 저렴하지만, 생체 거부반응, 밀착성 결여 등의 문제점과 피부조직의 기능을 대신할 수 없다는 한계를 가진다. 이러한 단점을 극복하기 위해 전기방사법으로 제작한 3 차원 구조의 합성고분자 지지체에 아시아티코사이드를 내포시킨 메쉬를 제작하였다. 이 후 제작된 메쉬의 형태적 특성 및 피부유래세포에 미치는 영향을 확인하여 3 차원 창상치유용 지지체로서의 가능성을

확인하였다. 실험 결과, 아시아티코사이드를 포함한 메쉬는 지지체로서 충분한 두께를 가지며 성인 진피섬유아세포에 독성을 나타내지 않고, 세포의 초기부착 및 증식을 촉진한다는 것을 확인하였다. 따라서 아시아티코사이드가 생체재료에 사용될 생리활성 물질로서 그 가치를 가짐을 확인할 수 있었다.

핵심되는 말 : 피부상처치유, 생리활성물질, 아시아티코사이드, 표피섬유세포, 진피섬유아세포, 세포거동, 인공피부.

PUBLICATION LIST

1. **Lee JH**, Kim HL, Lee MH, Taguchi H, Hyon SH, Park JC. Antimicrobial effect of medical adhesive composed of aldehyded dextran and ε-poly(L-lysine). J Microbiol Biotechnol 2011;21(11):1199-202.
2. Kim HL, **Lee JH**, Lee MH, Kim HH, Kim J, Han IH, *et al.* Direct-current treatment as a safe sterilization method for electrospun biodegradable polymer. Tissue Eng Regen Med 2011;8(3):320-5.
3. Kim HL, **Lee JH**, Lee MH, Kwon BJ, Park JC. Evaluation of electrospun (1,3)-(1,6)-β-D-glucans/biodegradable polymer as a artificial skin for full thickness wound healing. Tissue Eng 2012 (In press)
4. **Lee JH**, Kim HL, Lee MH, You KE, Kwon BJ, Seo HJ, Park JC. Asiaticoside enhances normal human skin cell migration, attachment and growth in vitro wound healing model. Phytomed 2012 (Accepted)